2.A.1 *Nuclear Physics* A267 (1976) 493–502; © *North-Holland Publishing Co., Amsterdam*

PRODUCTION OF NEGATIVE PIONS FROM HYDROGEN, DEUTERIUM AND CARBON BY HIGH-ENERGY ELECTRONS

F. H. HEIMLICH †, G. HUBER and E. RÖSSLE

Fakultät für Physik der Universität Freiburg/Breisgau

F. DAVID and H. MOMMSEN

Institut für Strahlen- und Kernphysik der Universität Bonn

and

D. WEGENER

Institut für Experimentelle Kernphysik der Universität und des Kernforschungszentrums Karlsruhe

Received 22 April 1976

Abstract: The yield of negative pions from $^1H_2$, $^2H_2$ and ^{12}C has been measured at 13° for incident electron energies between 2.68 and 6.0 GeV. Pion momentum spectra ranging from 0.7 to 3 GeV/c are presented and compared with simple production models. The measured $^{12}C/^1H$ ratios are well reproduced by calculated values for the nuclear transparency of carbon.

E NUCLEAR REACTIONS $^1H(e, \pi^-X)$, $^2H(e, \pi^-X)$, $^{12}C(e, \pi^-X)$, E = 2.68, 3.5, 4.5, 5, 6 GeV; measured negative pion $\sigma(E)$; deduced nuclear transparency. Liquid ^1H, ^2H targets.

1. Introduction

After the first experiments it was an open question whether the nuclear production of pions by real photons is dominated by surface production, leading to a $A^{\frac{2}{3}}$ dependence [1]), or by volume production. In more recent experiments, exponents between 0.72 and 0.83 were found, depending on the pion momentum [2]). This supports the assumption of a pion production uniformely distributed over the nuclear volume with subsequent interaction of pions with the nucleons of the nucleus [3]).

It is an interesting problem, which processes contribute to that interaction and which form of energy dependence results. In the region of the 3-3 resonance the data are not very well described by optical potential calculations [4]). In the present study it is attempted to examine the pion reabsorption process above the region of the 3-3 resonance for deuterons and ^{12}C nuclei. As primary particles we used electrons in the GeV range in connection with thin (about 0.003 radiation lengths) hydrogen,

† Present address: MIT, Cambridge, USA.

deuterium and carbon targets. The resulting spectrum of nearly real photons allows for single pion production as well as multipion production. Thus, we used the measured pion momentum as a parameter for the cross-section comparison between the yield from $^2H_2$ and ^{12}C and the reference reaction from $^1H_2$.

Furthermore, the presented data give the dependence of the π^- production cross section on pion momentum and incident energy for electron beams at 2.68, 3.5, 4.5, 5 and 6 GeV. This may also be useful for pion beam design and background estimates. Similar measurements have been done by Boyd [5]) at 500 MeV and by Boyarski *et al.* [6]) at 16 GeV.

2. Experimental method

A slowly ejected electron beam was produced by the Deutsches Elektronen-Synchrotron (DESY) with energies between 2.68 and 6 GeV and an energy resolution of about ± 0.5 %. The intensity was monitored by a secondary emission monitor and a totally absorbing Faraday cup. The targets were (a) a cylindrical cell of 30 mm diameter (0.025 mm Kapton H), filled with liquid hydrogen or deuterium, (b) a 1 ± 0.01 mm thick graphite plate with a density of 1.80 ± 0.025 g/cm^3.

The pions were detected at a fixed angle of 13°. The spectrometer consisted of a magnet with a homogeneous field, four wire spark chambers, three scintillation trigger counters, a threshold Čerenkov counter and a lead-scintillator-shower counter to separate pions from electrons. The horizontal aperture of the spectrometer was 1.57°, the solid angle 0.695 msr. The momentum acceptance was ± 20 % with a mean momentum resolution of ± 0.6 %. The upper limit (3 GeV/c) in the momentum of the detected pions was given by the maximum field (20 kG) of the spectrometer magnet, the lower limit (0.7 GeV/c) by the decreasing efficiency of the trigger counters. The spectrometer has been previously described in detail [7]).

3. Data reduction and corrections

An event was defined by coincident pulses from the three scintillator trigger counters Sc_1, Sc_2 and Sc_3. Electrons were suppressed off-line by an anticoincidence requirement for the Čerenkov counter C. Thus, the resulting trigger condition was $Sc_1 \cdot Sc_2 \cdot Sc_3 \cdot \bar{C}$. A typical pulse height spectrum of the shower counter S with the above trigger condition is shown in fig. 1. In addition to the prominent pion peak there is a second peak at larger pulse heights. A small part (3 %) of this latter peak is due to electrons which have produced a shower but not a pulse in the Čerenkov counter. The main part, however, is produced by pion-induced showers, especially by charge exchange processes, e.g.

$$\pi^- + p \rightarrow n + \pi^0 \\ \qquad\qquad\qquad\quad \big\lfloor\!\!\rightarrow 2\gamma,$$

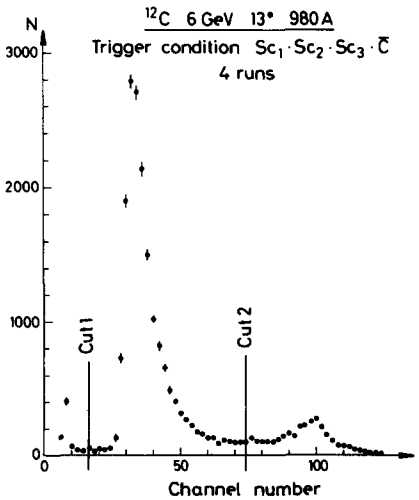

Fig. 1. Shower counter pulse height spectrum at 6 GeV electron energy. Pion momentum range between 1.4 and 2.4 GeV/c.

in the spectrometer material. Since the efficiency of "absorbed" pions for producing a shower depends critically on the pion energy and the spectrometer geometry we chose the following method for the cross-section evaluation: A cut (cut 2) in the region of the minimum between the two peaks eliminated the above mentioned Čerenkov-inefficient electrons and pion induced showers. The corresponding loss was taken into account by correcting the main peak for all possible absorption processes (see below). Another cut (cut 1) suppressed the noise in the shower counter at small pulse heights.

The main corrections applied were:

(a) Empty target rate (no target rate in the case of ^{12}C). In each bin an empty target rate was subtracted. It was calculated from the measured full/empty ratios under the trigger condition $Sc_1 \cdot S \cdot \bar{C}$. Typical values were 20–25 %.

(b) Spectrometer momentum acceptance: Only a few bins on each spectrometer setting have had to be corrected using a measured standard momentum acceptance function down to the 50 % range.

(c) Pion decay in flight: The loss due to decaying pions was ranging from 4 % at 3 GeV/c to 15 % at 0.7 GeV/c.

(d) The nuclear pion absorption: Using the data of Allardyce *et al.* [8]) the nuclear absorption of negative pions in the spectrometer material was calculated to be between 25 and 27 %.

(e) Trigger counter efficiency: The loss due to the combined inefficiencies of the three trigger counters was 4 % at 4 GeV/c to 12 % at 0.7 GeV/c.

(f) Spark chamber efficiency: The loss due to the spark chamber inefficiencies was 2 % at all momenta.

(g) Čerenkov efficiency for pions: The rate of pions misidentified as electrons in the Čerenkov counter is always smaller than 2 % up to 2.1 GeV/c. Above this value there is a steep rise in this correction up to 38 % at 3 GeV/c.

The K^- production rate is small compared with the π^- production and has been neglected.

4. Results and discussion

The data are presented in figs. 2 to 6 in form of double differential cross sections

$$d^2\sigma/d\Omega dp_\pi,$$

depending on the pion momentum p_π. The error bars shown are purely statistical, derived by combining the statistical errors of full and empty target rates. For most points, these errors are 2 to 10 %. There is an additional systematic error due to the uncertainties inferred from the setting of the cuts and the absorption, decay and efficiency corrections. It is estimated to be ± 8 % for all momenta up to 2.5 GeV/c For higher momenta this error may rise up to ± 20 %, caused mainly by large errors in Čerenkov pion efficiency. The error in the absolute cross-section scale, mainly

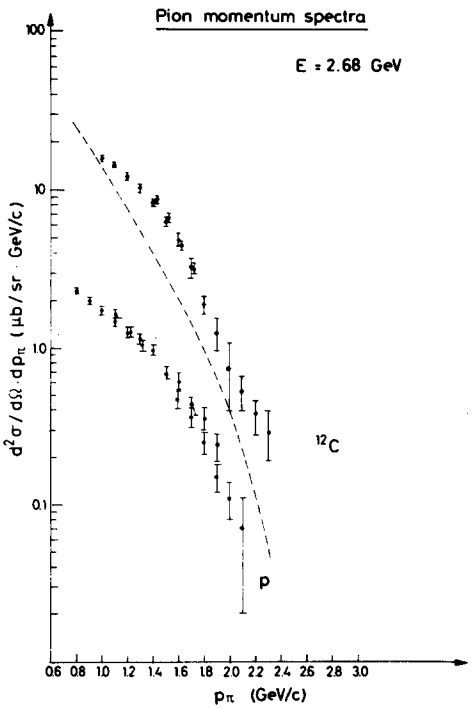

Fig. 2. Double differential cross section for the production of negative pions as a function of the pion momentum at an electron energy of 2.68 GeV. Targets: ^{12}C and p. Broken line: Drell model for ^{12}C, multiplied by a factor 25.

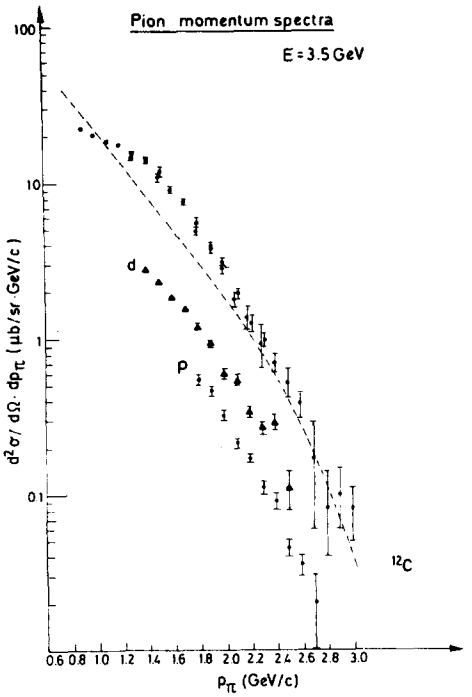

Fig. 3. Same as fig. 2, at 3.5 GeV for ^{12}C, d and p.

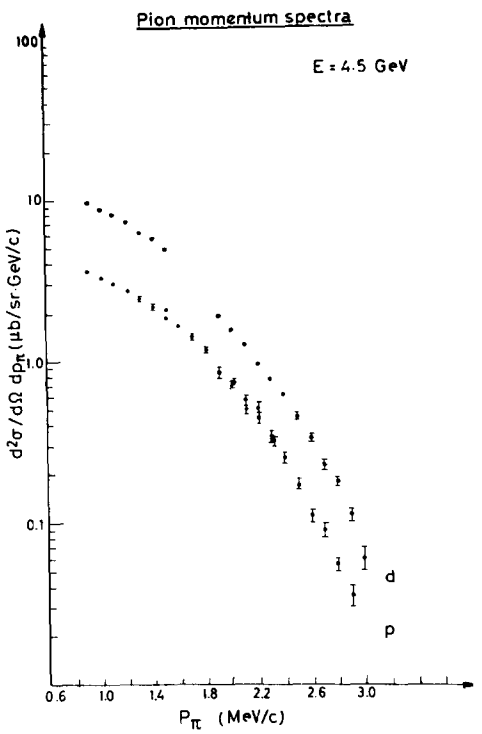

Fig. 4. Same as fig. 2, at 4.5 GeV for d and p, except the Drell model curve.

due to collected charge, target thickness and target density uncertainties, is estimated to be $\pm 10\,\%$.

In figs. 5 and 6 the momentum distribution of negative pions from photoproduction on hydrogen [9]) is shown for comparison. The curves are smoothed experimental distributions, obtained in a lab angle interval of 10° to 20° with a maximum bremsstrahlung energy of 5.8 GeV. They are normalized to our data at a pion momentum of 0.8 GeV/c. There is good agreement up to 2.5 GeV/c.

As far as we can draw conclusions from the data covering an angle interval of 1.57°, the angular distributions are relatively flat and exhibit the same trends as the photoproduction data on hydrogen [9]). There is no noticeable change in the slope of the angular distribution if we compare the $^1H_2$ data with the $^2H_2$ and ^{12}C data.

Furthermore, our results are compared with a π-production model due to Drell [10]) and a model for coherent photoproduction of ρ-mesons [6]). As in ref. [6]), the models yield much smaller cross sections than found in the experiment for almost all pion momenta.

The broken lines in figs. 2, 3, 5 and 6 represent a calculation for ^{12}C using the Drell model in connection with the photon spectrum of ref. [12]) and a π^+C total cross section of 304 mb [ref. [14])], multiplied with an arbitrary normalisation factor 25.

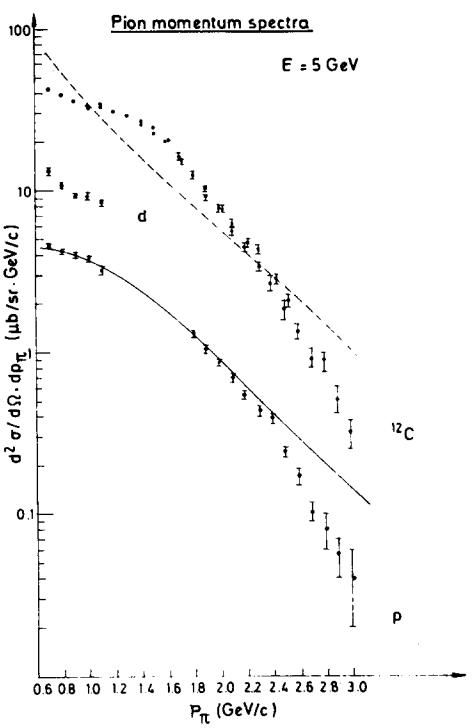

Fig. 5. Same as fig. 2, at 5 GeV for ^{12}C, d and p. Solid line: bubble chamber measurement [9]) for protons, normalized at 0.8 GeV/c.

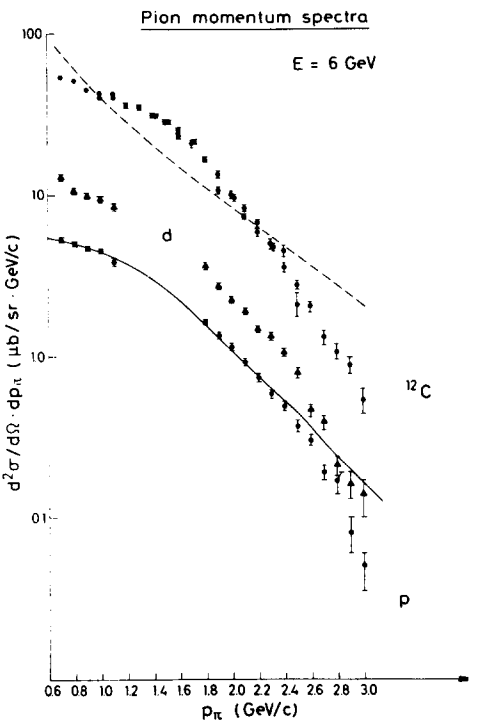

Fig. 6. Same as fig. 2, at 6 GeV for ^{12}C, d and p. Solid line: same as in fig. 5.

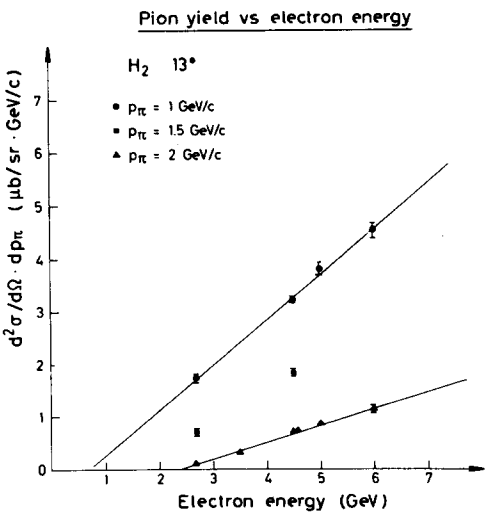

Fig. 7. Double differential cross section for the production of negative pions as a function of the primary electron energy at pion momenta 1, 1.5 and 2 GeV/c. The straight lines are only shown to guide the eye. Target: protons.

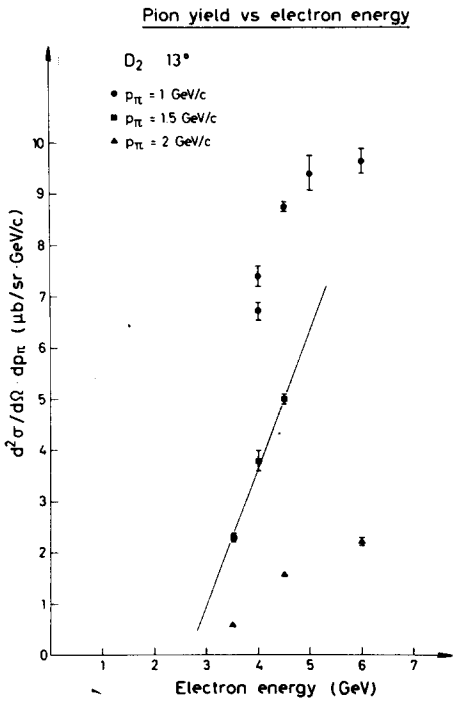

Fig. 8. Same as fig. 7 for deuterons.

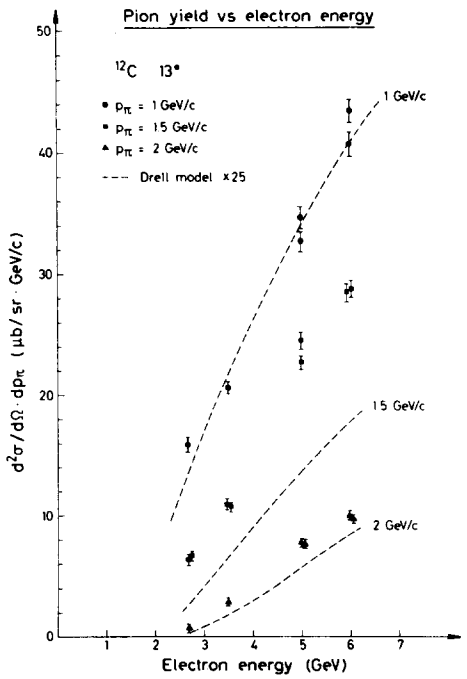

Fig. 9. Same as fig. 7 for ^{12}C. Broken lines: Drell model, multiplied by a factor 25.

The comparison of our data with the theoretical prediction shows that the shape of the spectra is roughly reproduced.

In figs. 7 to 9 the dependence of the pion production cross section from the primary energy is shown for $^1H_2$, $^2H_2$ and ^{12}C. The yields seem to increase linearly with the electron energy. The straight lines are only shown to guide the eye. The broken line in fig. 9 represents again the Drell model result, multiplied by a factor 25. The increase of the pion production with increasing electron energy is roughly reproduced.

In fig. 10, the carbon to proton and deuteron to proton cross-section ratios are given for all electron energies as a function of the pion momentum p_π.

The deuteron ratios are almost always larger than 2.0 indicating that the π^- yield from the neutron is higher than from the proton. This is probably due to the single π^- production part $\gamma_v + n \rightarrow \pi^- + p$. The production of a single π^- by a virtual photon is possible on a neutron, but not on a proton. The ratios $^{12}C/^1H$ are much lower than six times the $^2H/^1H$ ratio and even lower than the value 12 for twelve hypothetical protons. This suggests a strong reabsorption of the produced pions in the rest nucleus.

The $^2H/^1H$ ratios for low primary energies are higher than those for high primary energies, especially in the low pion momentum region. An explanation is the increase

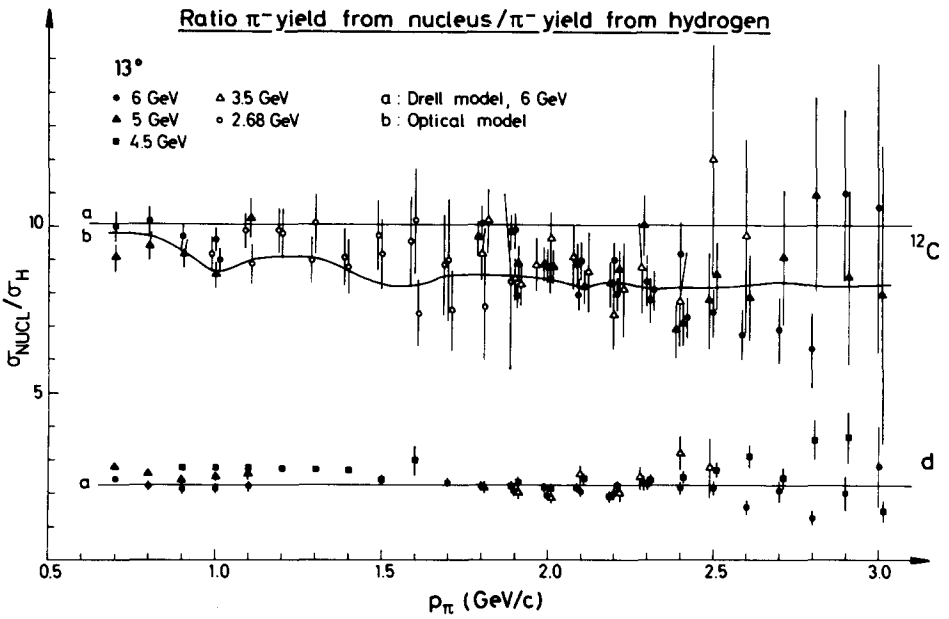

Fig. 10. Cross sections for ^{12}C and d, divided by the reference cross section for protons, as a function of the pion momentum. All measured electron energies are included. Theoretical curves: (a) Drell model at 6 GeV. (b) Optical model calculation for ^{12}C/^{1}H, described in the text.

of the single-pion production compared to the multipion production for lower photon energy. This trend is reproduced, although not in absolute magnitude, by the Drell model [10]).

We are aware of the fact that the graph used by Drell may not give the main contribution to the process, but $\gamma + p \rightarrow \pi^- + \Delta^{++}$ might dominate in the lower part of the momentum region considered [11]). This cross section has, however, not yet been calculated for nuclear systems. Because of this we applied the Drell model to calculate the curve (a) for deuterons in fig. 10 at 6 GeV electron energy. For this the measured π^+p and π^+d total cross sections [12]) were averaged over an assumed $1/K$ form of the spectrum of nearly real photons [13]). The almost constant result (averaged 2.24) agrees well with our 6 GeV data.

There is no marked dependence on the primary energy in the ^{12}C/^{1}H ratios. From that it may be concluded that final state effects are more important than the difference between the production cross section on photons and neutrons. Using the π^+C total cross-section value of 304 mb at 2.01 GeV/c [ref. [14])] and assuming a constant total cross-section ratio (π^+ ^{12}C)/(π^+ ^{1}H) we obtain the Drell model line (a) for carbon in fig. 10 at a value of 10.1.

A more elaborate model for the nuclear transparency to photoproduced pions has been published by De Carvalho *et al.* [15]). They use an optical model and assume an equivalent uniform distribution for the nuclear density. The interaction of the

photoproduced pions is described in terms of collisions with free nucleons within a nucleus. Extending this model to the pion momenta up to 3 GeV/c and using the measured inelastic (total minus elastic) πN cross sections [12]) we obtain curve (b) in fig. 10. A normalisation factor of 2.2 for the ^{2}H/^{1}H ratio has been used in this calculation. This is justified by the experimental result for the inclusive π^- ratio from neutrons to protons [16]):

$$\frac{\sigma(\gamma n, \pi^- X)}{\sigma(\gamma p, \pi^- X)} = 1.2 \frac{\sigma(\gamma n, \pi^+ X)}{\sigma(\gamma p, \pi^- X)}.$$

The charge symmetric cross sections $\sigma(\gamma n, \pi^+ X)$ and $\sigma(\gamma p, \pi^- X)$ are found to be equal for multipion production [17]), that is, no isospin interference effects have been observed in that case. Since the coherent production on the deuteron is expected to be small [16]) and final state effects are estimated to be smaller than 5 % [ref. [18])], we may write: $\sigma(\gamma d, \pi^- X) = \sigma(\gamma p, \pi^- X) + \sigma(\gamma n, \pi^- X)$. Combining these results, we obtain $\sigma(\gamma d, \pi^- X)/\sigma(\gamma p, \pi^- X) = 2.2$, in good agreement with the data.

The optical model curve (b) for the ^{12}C/^{1}H ratios in fig. 10 calculated as described above is in very good agreement with the experimental data. From this we may conclude that the optical model is adequate for the absorption of volume-produced negative pions with momenta of a few GeV/c, at least in the case of ^{12}C. Neither energy shifts due to elastic processes nor hadronic "shadowing" of the nearly real incoming photons – which is possible, but not necessary – seem to be essential.

We thank the DESY laboratory for its hospitality and its support. The untiring assistance of Ing. H. Sindt was of greatest importance for this experiment. We are further indebted to Dr. J. Bleckwenn for help in taking the data and Dr. H. Meyer for valuable discussions. This work has been supported by the Bundesministerium für Forschung und Technologie.

References

1) S. T. Butler, Phys. Rev. **87** (1952) 1117
2) N. V. Goncharov, A. I. Derebchinskii, O. G. Konovalov, S. G. Tonapetyan and V. M. Khvorostyan, Sov. J. Nucl. Phys. **17** (1973) 124;
B. I. Shramenko, I. A. Grishaev, V. I. Nikiforov and G. D. Pugachev, Kharkov Phys. Tech. Inst. KhFTI 73-31 (1973) p. 74
3) V. Di Napoli, Nuovo Cim. Lett. **12** (1975) 609
4) A. V. Shebeko and N. V. Goncharov, Sov. J. Nucl. Phys. **18** (1974) 532
5) D. Boyd, Stanford Univ. HEPL 657 (1972)
6) A. Boyarski, F. Bulos, W. Busza, D. Coward, R. Diebold, J. Litt, A. Minten, B. Richter and R. Taylor, Phys. Rev. Lett. **18** (1967) 363
7) J. Moritz, K. H. Schmidt, D. Wegener, J. Bleckwenn and E. Engels, Jr., Nucl. Phys. **B41** (1972) 336; S. Galster, G. Hartwig, H. Klein, J. Moritz, K. H. Schmidt, W. Schmidt-Parzefall and D. Wegener, Phys. Rev. **D5** (1972) 519
8) B. W. Allardyce, C. J. Batty, D. J. Baugh, E. Friedman, G. Heymann, M. E. Cage, G. J. Pyle, G. T. A. Squier, A. S. Clough, D. F. Jackson, S. Murugesu and V. Rajaratnam, Nucl. Phys. **A209** (1973) 1

9) U. Brall, R. Erbe, G. Reimann, E. Schüttler, W. Bothin, H. Böttcher, K. Lanius, A. Meyer, A. Pose, J. Schreiber, K. Böckmann, W. Johnssen, J. Moebes, H. Mück, B. Nellen, W. Tejessy, G. Harigel, G. Horlitz, E. Lohrmann, H. Meyer, W. P. Swanson, M. W. Teucher, G. Wolf, S. Wolff, D. Lüke, D. Pollmann, P. Söding, H. Spitzer, H. Beisel, H. Filthuth, H. Kolar, P. Steffen, P. Freund, N. Schmitz, J. Seyerlein and P. Seyboth, Nucl. Phys. **B1** (1967) 668
10) S. D. Drell, Phys. Rev. Lett. **5** (1960) 278
11) D. Lüke and P. Söding, Springer Tracts in Modern Physics **59** (1971) 39
12) E. Bracci, J. P. Droulez, E. Flaminio, J. D. Hansen and D. R. O. Morrison, CERN/HERA 72-1 (1972)
13) G. R. Bishop, in Nuclear structure and electromagnetic interactions, ed. N. MacDonald (Plenum Press, New York, 1965) p. 211
14) B. Gobbi, W. Hakel, J. L. Rosen and S. Shapiro, Phys. Rev. Lett. **29** (1972) 1278
15) H. G. De Carvalho, J. B. Martins, O. A. P. Tavares, R. A. M. S. Nazareth and V. Di Napoli, Nuovo Cim. Lett. **2** (1971) 1139; **4** (1972) 365
16) J. Gandsman, G. Alexander, S. Dagan, L. D. Jacobs, A. Levy, D. Lissauer and L. M. Rosenstein, Nucl. Phys. **B61** (1973) 32
17) R. Schiffer, H. H. J. Schnackers, V. Valdmanis, U. Idschok, K. Müller, P. Benz, R. Riebensahm, V. Schulz, F. Storim, G. Ullrich, G. Knies, O. Braun, J. Stiewe, H. Finger, C. Kiesling, P. Schlamp and J. Weigl, Nucl. Phys. **B38** (1972) 628
18) Y. Sumi, Prog. Theor. Phys. **41** (1969) 1227